

E-ISSN: 2664-7583 P-ISSN: 2664-7575 Impact Factor (RJIF): 8.12 IJOS 2025; 7(2): 368-372 © 2025 IJPA

www.physicsjournal.in Received: 18-10-2025 Accepted: 17-11-2025

#### Dr. Raj Kumari

Assistant Professor, Department of Physics, Government College for Women, Shahzadpur, Ambala, Haryana, India

# Probing the impact of nuclear surface energy coefficient on the halo-induced fusion reactions

## Raj Kumari

**DOI:** https://www.doi.org/10.33545/26647575.2025.v7.i2e.213

#### Abstract

Halo nuclei, known for their unexpectedly large sizes as compared to their isobars, don't obey nuclear shell model expectations. Their significant deviations from the expected nuclear structures have established them as an interesting area of research. The extended matter distribution due to weakly-bound nucleons significantly increases their nuclear surface area. This enhanced surface area and lower binding of halo nucleons significantly affect the surface energy coefficient  $(\gamma)$  as compared to that for a non-halo nucleus. This surface energy coefficient accounts for the energy associated with the interaction between the surfaces of the two colliding nuclei. The lower surface energy contributes to lower binding energy and thus exotic behavior of halo nuclei. Our earlier study on the halo structure effects on the fusion probabilities unveiled that the extended halo radii significantly affect the fusion barrier as well as fusion probabilities. In the present paper, the impact of the surface energy coefficient on the fusion probabilities has been discussed in the halo-induced fusion reactions by employing a proximity-based potential. Neutron-halo ( $^6$ He) and proton-halo ( $^8$ B) induced fusion reactions have been considered for the present study.

**Keywords:** Halo nucleus, neutron-halo, proton-halo, surface energy coefficient, proximity-based potential, fusion cross-section

### 1. Introduction

The developments in the radioactive-ion beams (RIBs) in the last few decades have facilitated us to investigate many unexplored nuclei in the nuclear chart away from the line of stability. At the farther end of the line of stability, the separation energy of the last nucleon decreases and becomes zero at the drip line. The drip line separates the stable nuclei from the unstable nuclei as the nuclei at the drip line lose their capacity to hold any extra nucleon. Halo nuclei are found to be close or even lying on the neutron drip line. A halo nucleus, as the name proposed by Hansen and Jonson [1, 2], is composed of a core and extremely loosely-bound nucleons in the classically forbidden region around it. These halo neutrons/protons are more probable at distances much larger than the usual nuclear radius and hence, have very little binding energy. A stable nucleus has an average nucleon separation energy of about 6-8 MeV, which, however, in the case of a halo nucleus is found to 1 MeV. The valence nucleons in these exotic nuclei, due to their lower separation energy, can easily tunnel far into the classically forbidden region and therefore, extend the nuclear density up to large distances. The <sup>6</sup>He, <sup>11</sup>Li and <sup>11</sup>Be nuclei are widely studied neutron-halo nuclei due to availability of these beams with good intensity and variable energies. In addition to neutron halos, other nuclei at drip line are protons halos, which have one or more loosely bound protons. Protonhalos are less abundant due to the repulsive Coulomb field. Some of the proton-halo nuclei are <sup>8</sup>B, <sup>17</sup>F etc. Our studies <sup>[3, 4]</sup>, revealed that the extended size is a decisive factor for increasing the fusion outcome in the reactions induced by proton-halo projectiles. However, size effects mainly contribute in the break-up process or transfer process in preference to the fusion yield in case of the fusion reactions induced by neutron-halo projectiles. Hence, the type of the halo nuclei i.e. proton halo or neutron halo decides the impact of halo structures on the fusion probabilities.

In a study by my co-workers Dutt and Puri [5] and later by Gharaei and Ghodsi [6, 7], the impact of surface energy coefficient on the fusion barrier has been revealed. These studies showed that different values of surface energy coefficients significantly affect the barriers of fusion reactions induced by strongly as well as weakly bound projectiles.

Corresponding Author: Dr. Raj Kumari

Assistant Professor, Department of Physics, Government College for Women, Shahzadpur, Ambala, Haryana, India The impact of surface energy coefficient has also been discussed in  $\alpha$ -decay as well as on one-proton radioactivity using proximity-based potentials [8, 9]. Motivated by these studies, we have attempted to probe the impact of nuclear surface energy coefficient in the fusion reactions involving neutron-halo ( $^6$ He) and proton-halo ( $^8$ B) projectiles.

This paper is structured in the following way: The next part describes the research methodology, accompanied by the results and summary.

### 2. Methodology

The present study is carried out using Aage Winther Potential (AW 95), which is a proximity-based potential  $^{[10,\ 11]}$ . Here, the nuclear potentials  $V_N$  (R) are parameterized in the proximity fashion  $^{[12]}$ , where the nucleus-nucleus potential is expressed as a product of a geometrical factor and a universal function. The geometrical factor depends on the masses of the colliding nuclei, whereas the universal function is independent of the features of the colliding nuclei and instead, it depends on the separation distance between two colliding nuclei (s).

These proximity-based potentials have been successfully employed for studying symmetric as well as asymmetric colliding nuclei and sub-barrier fusion also [13-16].

The total interaction potential  $V_T(R)$  is calculated by adding Coulomb potential  $V_C(R)$  to the nuclear interaction potential  $V_N(R)$ .

$$V_T(R) = V_N(R) + V_C(R),$$
(1)

Here

$$V_C(R) = \frac{1.44 \times Z_1 \times Z_2}{R} \tag{2}$$

and  $Z_1$  and  $Z_2$  are the atomic numbers of the colliding nuclei. In this study, the nuclear potential due to Aage Winther is used.

## 2.1 Aage Winther Potential (AW 95)

According to Aage Winter [10], the nucleus-nucleus interaction potential is written as:

According to Aage Winter [10], the nucleus-nucleus interaction potential is written as:

$$V_N^{AW~95}(R) = -\frac{R_1 R_2}{R_1 + R_2} \times \frac{16\pi\gamma a}{1 + \epsilon \frac{R - R_0}{a}} \text{ MeV}.$$
 (3)

Where, the surface diffuseness factor "a" reads as

$$a = \left[ \frac{1}{1.17 \left[ 1 + 0.53 \left( A_1^{-\frac{1}{3}} + A_2^{-\frac{1}{3}} \right) \right]} \right] \text{fm}, \tag{4}$$

$$And R_0 = (R_1 + R_2) \text{ fm}, (5)$$

The nuclear radius  $R_i$  (i = 1, 2) is given by

$$R_i = \left(1.20 \ A_i^{\frac{1}{8}} - 0.09\right) \text{fm.} \tag{6}$$

The expression for the surface energy coefficient  $(\gamma)$  is given by

$$= 0.95 \left[ 1 - 1.8 \left( \frac{A_1 - 2Z_1}{A_1} \right) \left( \frac{A_2 - 2Z_2}{A_2} \right) \right]_{MeV} fm^2, \tag{7}$$

Where  $A_i$  and  $Z_i$  corresponds to mass number and proton number of both colliding nuclei.

In the present study, different values of surface energy coefficients ( $\gamma$ -MN76,  $\gamma$ -MN95,  $\gamma$ -MS00 and  $\gamma$ -PD03) have been used in the proximity-based potential due to AW 95 to account for different surface energy effects. These modified versions of AW 95 are described below:

- **2.2 AW 95 (\gamma-MN76):** This modified version utilizes the values of surface energy coefficient given by Möller and Nix <sup>[17]</sup>. Here  $\gamma_0 = 1.460734$  MeV/fm<sup>2</sup> and  $K_s = 4.0$ .
- **2.3 AW 95 (\gamma-MN95):** Later on, values of  $\gamma_0$  and  $K_s$  were refitted by using better mass formula due to Möller *et al.* <sup>[18]</sup>. This new set of values reads as  $\gamma_0 = 1.25284$  MeV/fm<sup>2</sup> and  $K_s = 2.345$ .
- **2.4 AW 95 (\gamma-MS00):** This modified version uses the form of surface energy coefficient given by Myers and Swiatecki <sup>[19]</sup>. This form of surface energy coefficient depends upon the neutron skin of the two colliding nuclei.
- **2.5 AW 95** ( $\gamma$ -**PD03**): This modified version utilizes the surface energy coefficients given by Pomorski and Dudek <sup>[20]</sup>, which also includes different curvature effects in the liquid drop model. This study provided the values of 1.08948 MeV/fm<sup>2</sup> and 1.9830 for coefficients  $\gamma_0$  and  $K_s$ , respectively.

## 3. Results and Discussion

The barrier heights are calculated by using these different values of surface energy coefficients with standard radii in AW 95 nuclear potential for the reactions of  $^6{\rm He}$  +  $^{209}{\rm Bi}$  and  $^8{\rm B}$  +  $^{58}{\rm Ni}$  and then by including halo radii extracted from the cross-section measurements  $^{[21]}$  (AW 95<sup>halo</sup>) and are listed in Table 1. In AW 95<sup>halo</sup> nuclear potential, halo radii of proton and neutron-halo nuclei are used instead of standard radii.

From Table 1, we see that the fusion barrier heights are lowest for the cases with largest value of surface energy coefficient *i.e.* for AW 95 ( $\gamma$ -MN76). This trend is observed in both cases *i.e.* calculations involving standard radius as well as halo radius. Also, the barrier heights corresponding to the halo radius are lower compared to those in the case of standard radius.

Table 1: The calculated barrier heights (in MeV) for the reactions induced by neutron- and proton-halo projectiles corresponding to different modified versions (including different values of surface energy coefficient  $\gamma$ ). Calculations for standard radii nuclei are done by using AW 95, whereas calculations in halo nuclei case are done by using AW 95<sup>halo</sup>.

Reaction	AW 95 Standard V <sub>B</sub>	AW 95 (γ-MN76) V <sub>B</sub>	AW 95 (γ-MN95) <b>V</b> <sub>B</sub>	AW 95 (γ-MS00) <b>V</b> <sub>B</sub>	AW 95 (γ-PD03) <b>V</b> <sub>B</sub>
Standard Radius					
${}_{2}^{6}$ He + ${}_{83}^{209}$ Bi	19.95	19.67	19.68	19.68	19.81
${}_{5}^{8}B + {}_{28}^{58}Ni$	21.10	20.41	20.66	20.88	20.88
Halo Radius					
${}_{2}^{6}$ He + ${}_{83}^{209}$ Bi	18.66	18.42	18.43	18.42	18.54
${}_{5}^{8}B + {}_{28}^{58}Ni$	20.55	19.89	20.13	20.34	20.34

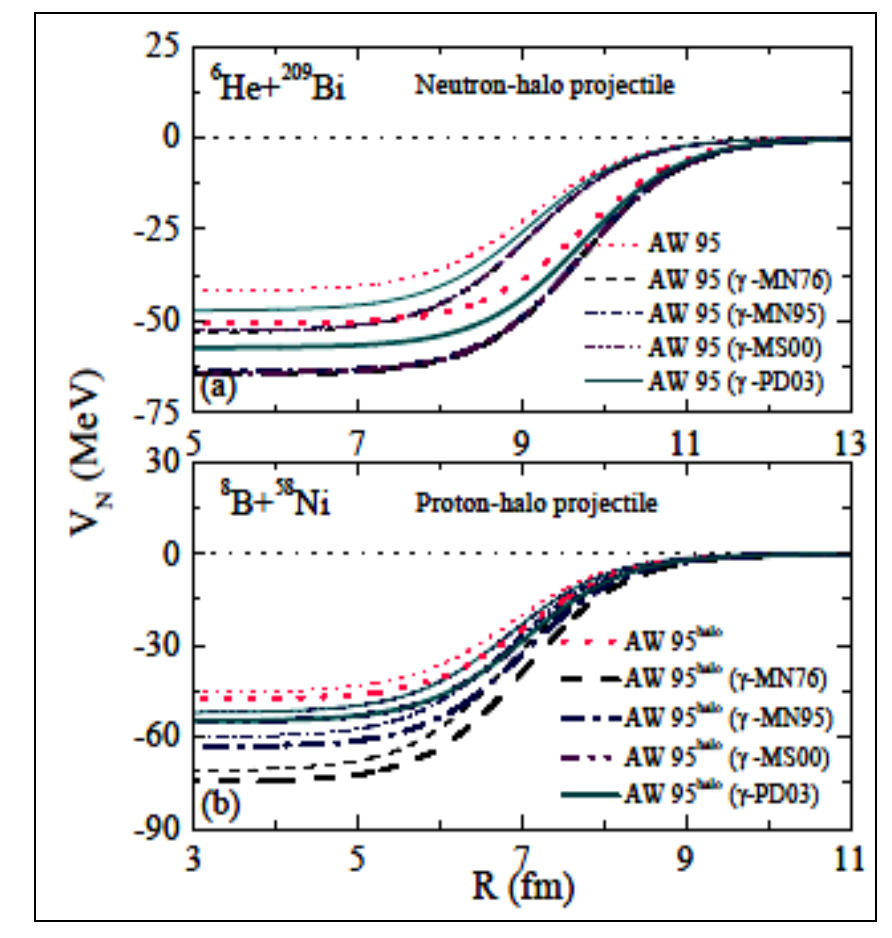
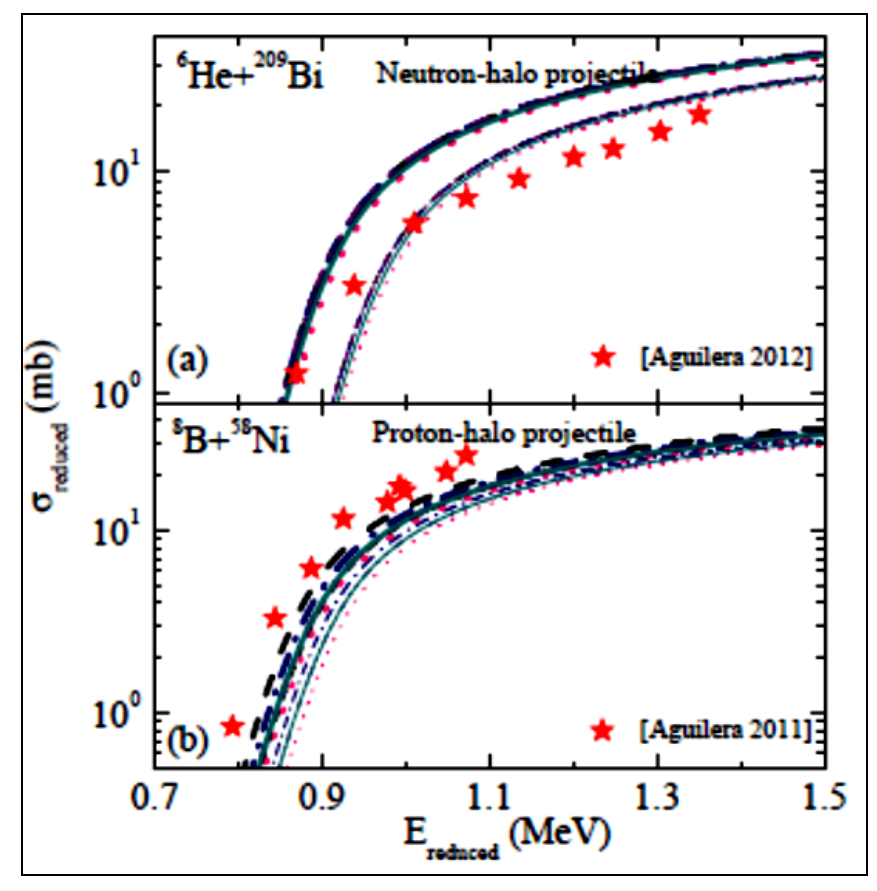


Fig 1: The dependence of the nuclear potential V<sub>N</sub> (MeV), calculated using various modified versions of AW 95 and AW 95<sup>halo</sup>, on the internuclear distance R (fm) is presented for <sup>6</sup>He +<sup>209</sup>Bi and <sup>8</sup>B +<sup>58</sup>Ni reactions. Different symbols used here, are explained in the text

In Figure 1 (a) and (b), the dependence of the nuclear potentials V<sub>N</sub> (MeV) on the inter nuclear distance R (fm) is displayed for the reactions of <sup>6</sup>He + <sup>209</sup>Bi and <sup>8</sup>B + <sup>58</sup>Ni, respectively. The pink (dotted), black (dashed), navy (dashdotted), purple (dash-double dotted) and dark cyan (solid) thin and thick lines correspond to calculations using standard radius and halo radius, respectively, in AW 95, AW 95 (γ-MN76), AW 95 (γ-MN95), AW 95 (γ-MS00) and AW 95 (γ-PD03). In Fig. 1 (a), AW 95 (with  $\gamma = 0.830$ ) leads to shallowest nuclear potential compared to other versions and AW 95 ( $\gamma$ -MN76) (with  $\gamma = 1.060$ )/AW 95 ( $\gamma$ -MS00) (with  $\gamma$ = 1.055) give deepest nuclear potential. This is due to the reason that larger value of the surface energy coefficient corresponds to more surface tension and hence, more attraction. However, when the halo radius deduced from the cross-section measurements for <sup>6</sup>He is included in the calculations i.e. AW 95<sup>halo</sup>, the nuclear potentials corresponding to different versions of surface energy coefficients are significantly lowered. This is due to the fact

that halo radius of <sup>6</sup>He nucleus (i.e. 2.71 fm, deduced from measurements [21]) is large compared to its standard radius (i.e. 2.09 fm, calculated using AW 95). Due to large halo radius, the nuclear forces start acting even at larger distances and hence, resulting in deeper nuclear potential. Therefore, we find that largest value of surface energy coefficient and inclusion of halo radius lead to deepest nuclear potential and hence, lowest barrier height for the reaction of <sup>6</sup>He + <sup>209</sup>Bi. Similar study is also conducted for the fusion reaction of <sup>8</sup>B + <sup>58</sup>Ni involving proton-halo projectile (shown in Figure 1 (b)). The observed trends are similar to that in earlier case, but the changes observed in the depth of nuclear potential in this case is less. This is because, the surface energy coefficient also depends upon the asymmetry parameter (I), which is zero in case of <sup>8</sup>B + <sup>58</sup>Ni and is non-zero (i.e. 0.21) in the case of <sup>6</sup>He + <sup>209</sup>Bi. Moreover, the difference between the halo radius of <sup>8</sup>B nucleus (i.e. 2.50 fm, deduced from measurements <sup>[21]</sup>) and its standard radius (i.e. 2.31 fm, calculated using AW 95) is less compared to that in <sup>6</sup>He case.



**Fig 2:** The reduced fusion cross-sections are presented as a function of reduced center of mass energies for the reactions of  ${}^{6}\text{He} + {}^{209}\text{Bi}$  and  ${}^{8}\text{B} + {}^{58}\text{Ni}$ . The experimental data for  ${}^{6}\text{He} + {}^{209}\text{Bi}$  reaction is taken from Aguilera 2012 [23] and for  ${}^{8}\text{B} + {}^{58}\text{Ni}$  reaction is taken from Aguilera 2011 [22]. Various lines have the same meaning as in Figure 1.

In Figure 2 (a) and (b), the reduced fusion cross sections  $\sigma$  reduced (mb) are displayed as a function of reduced center of mass energy,  $E_{reduced}$  (MeV) for the reactions of  $^6\text{He}+^{209}\text{Bi}$  and  $^8\text{B}+^{58}\text{Ni}$ , respectively. We notice higher fusion cross sections corresponding to higher values of  $\gamma$  and these values are comparatively higher for the halo case. This is because, halo radius and largest value of  $\gamma$  give deepest nuclear potential and hence lowest Coulomb barrier. This results in enhanced fusion cross sections which are found to be closer to experimental data in case of  $^8\text{B}+^{58}\text{Ni}$  reaction, which is a proton-halo induced fusion reaction  $^{[22]}$ . However, in case of  $^6\text{He}+^{209}\text{Bi}$  reaction, which is a neutron-halo induced reaction, extended size effects contribute significantly to processes other than fusion and can be held responsible for deviation from the experimental data  $^{[23]}$ .

## 4. Summary

We investigated the impact of surface energy coefficient on the halo-induced fusion reactions by employing different modified versions of Aage Winther (AW 95) potential. From this study, we concluded that larger value of surface energy coefficient leads to deeper nuclear potential and enhanced fusion cross sections at all incident energies. This study revealed that surface energy coefficient plays a significant role in the halo-induced fusion reactions and contribute differently for reactions induced by neutron-halo as compared to for reactions induced by proton-halo projectiles.

## References

- 1. Hansen PG, Jonson B. The neutron halo of extremely neutron-rich nuclei. Europhys Lett. 1987;4:409-414.
- 2. Jonson B. Halo nuclei. Nucl Phys A. 1994;574(2):151-166.

- 3. Kumari R. Study of fusion probabilities with halo nuclei using different proximity-based potentials. Nucl Phys A. 2013;917:85-91.
- 4. Kumari R. Towards the fusion of weakly bound projectiles with heavy targets with proximity-based potentials. Eur Phys J Web Conf. 2014;69:00014.
- 5. Dutt I, Puri RK. Role of surface energy coefficients and nuclear surface diffuseness in the fusion of heavy ions. Phys Rev C. 2010;81:047601.
- 6. Gharaei R, Ghodsi ON. Role of surface energy coefficients and temperature in fusion reactions induced by weakly bound projectiles. Commun Theor Phys. 2015;64:185-196.
- Salehi M, Ghodsi ON. The role of surface energy coefficient in heavy-ion reactions and improved proximity model. Int J Mod Phys E. 2011;20(11):2337-2349.
- 8. Gharaei R, Ghal-Eh N, Haghighi K. Investigating the impact of nuclear surface energy coefficients on one-proton radioactivity. Phys Rev C. 2024;110:024603.
- 9. Rajeshwari NS, Balasubramanium M. Nuclear surface energy coefficients in α-decay. J Phys G Nucl Part Phys. 2013;40(3):035104.
- 10. Winther A. Dissipation, polarization and fluctuation in grazing heavy-ion collisions and the boundary to the chaotic regime. Nucl Phys A. 1995;594:203-245.
- 11. Denisov VY. Interaction potential between heavy ions. Phys Lett B. 2002;526:315-321.
- 12. Blocki J, Randrup J, Swiatecki J, Tsang CF. Proximity forces. Ann Phys. 1977;105:427-462.
- 13. Kumari R. A comparative study of sub-barrier fusion using proximity-based potentials. AIP Conf Proc. 2013;1524:139-142.

- 14. Dutt I, Puri RK. Systematic study of the fusion barriers using different proximity-type potentials for N=Z colliding nuclei: New extensions. Phys Rev C. 2010;81:044615.
- 15. Dutt I, Puri RK. Comparison of different proximity potentials for asymmetric colliding nuclei. Phys Rev C. 2010;81:064609.
- 16. Sharma MK, Puri RK, Gupta RK. Analytical description of heavy-ion potentials for collisions between nuclei of same shell. Eur Phys J A. 1998;2:69-75.
- 17. Möller P, Nix JR. Macroscopic potential-energy surfaces for symmetric fission and heavy-ion reactions. Nucl Phys A. 1976;272:502-32.
- 18. Möller P, Nix JR, Myers WD, Swiatecki WJ. Nuclear ground-state masses and deformations. At Data Nucl Data Tables. 1995;59:185-381.
- 19. Myers WD, Swiatecki WJ. Nucleus-nucleus proximity potential and superheavy nuclei. Phys Rev C. 2000;62:044610.
- 20. Pomorski K, Dudek J. Nuclear liquid-drop model and surface-curvature effects. Phys Rev C. 2003;67:044316.
- 21. Al-Khalili JS, Tostevin JA, Thompson IJ. Radii of halo nuclei from cross-section measurements. Phys Rev C. 1996;54:1843-52.
- 22. Aguilera EF. Near-barrier fusion of the 8B+58Ni protonhalo system. Phys Rev Lett. 2011;107:092701.
- Aguilera EF, Kolata JJ. Angular momentum limit for fusion of halo and weakly bound systems. Phys Rev C. 2012;85:014603.